6.0 MeV u^{-1} carbon ion (C^{6+} and C^{4+})-induced secondary electron emission from water vapor

2013 Phys. Scr. 2013 014039

(http://iopscience.iop.org/1402-4896/2013/T156/014039)

IOP PUBLISHING PHYSICA SCRIPTA

Phys. Scr. **T156** (2013) 014039 (5pp) doi:10.1088/0031-8949/2013/T156/014039

6.0 MeV u^{-1} carbon ion (C^{6+} and C^{4+})-induced secondary electron emission from water vapor

D Ohsawa[1], **H Tawara**[2], **F Soga**[3], **M E Galassi**[4] **and R D Rivarola**[4]

[1] Radioisotope Research Center, Kyoto University, Kyoto 606-8502, Japan
[2] National Institute for Fusion Science, Toki 509-5292, Japan
[3] National Institute of Radiological Sciences, Chiba 263-8555, Japan
[4] Instituto de Física Rosario, CONICET and Universidad Nacional de Rosario, Rosario, Argentina

E-mail: ohsawa.daisuke.2s@kyoto-u.ac.jp

Received 3 September 2012
Accepted for publication 20 January 2013
Published 23 September 2013
Online at stacks.iop.org/PhysScr/T156/014039

Abstract

We have precisely measured absolute double differential cross sections (DDCSs) for secondary electron emission produced in collisions of 6.0 MeV u^{-1} C^{6+} and C^{4+} ions with water vapor. Theoretical calculations of the DDCSs were made for C^{6+} ions using the continuum distorted wave-eikonal initial state model (CDW-EIS) in its straight-line version of the impact parameter approximation, showing general good agreement with experimental data, except in the intermediate- and high-energy region (>50 eV), particularly at the backward angles (>110°). On the other hand, the single differential cross section (SDCS), which was obtained by integrating the measured DDCSs over the solid angle, showed fairly good agreement with the CDW-EIS in the low-energy region (<200 eV), while a significant discrepancy between the observed SDCS and the Rudd-model scaling (×36) can be seen, suggesting that a simple Z^2-scaling law (i.e. first Born approximation) is not applicable for high-Z bare projectiles such as C^{6+} ions. The SDCS of C^{4+} ions was observed to be smaller than that of C^{6+} ions by ~50% in the low-energy region (<200 eV) due to the screening effect of its bound electrons in C^{4+} ions, which could be explained quantitatively by taking account of an effective projectile charge.

PACS number: 34.50.Gb

1. Introduction

Although secondary electron emission from water by ion impact has been of great interest in fields such as radiobiology and atomic physics, there are only a few data, particularly for heavy-ion impact with incident energies of several MeV u^{-1} or higher. Motivated by this situation, considerable effort has been invested into this study since 1994. Our previous papers [1, 2] reported in detail on an apparatus for measuring secondary electrons from water vapor, along with the deduction of experimental parameters such as target molecule density, energy resolution and transmission of the electron spectrometer and detection efficiency of the electron detector (MCP). The absolute double and single differential cross section (DDCS and SDCS) data obtained with He^{2+} ions were also discussed by comparing them with a simple Z^2-scaling of the semiempirical Rudd model and the modified Rutherford cross sections taking into account the binding energy of an electron ejected from each subshell of a water molecule. In emission angles, the measurements were carried out at 20–160° by 10° steps for both 6.0 and 10.0 MeV u^{-1} He^{2+} ions, while in electron energies, 7 eV–10 keV for 6.0 MeV u^{-1} and 20 eV–10 keV for 10.0 MeV u^{-1}. Subsequently, the measurements with 6.0 MeV u^{-1} C^{6+} ions were made at electron energies of 10 eV–1 keV. Theoretical investigations were also performed for these experimental DDCS and SDCS data, showing meaningful and significant discrepancies [3, 4]. Recent modifications allowed us to measure the DDCSs at electron energies down to 1 eV as well as to measure high-energy electrons (>1 keV) with low-background level.

In this paper, we present experimental DDCS and SDCS data for secondary electron emission from water vapor by the impact of 6.0 MeV u^{-1} C^{6+} and C^{4+} ions. The experimental data with C^{6+} ions are compared with the continuum distorted wave-eikonal initial state model (CDW-EIS). The screening effect of the bound electrons in C^{4+} ions is also discussed.

2. Experiment

An outline of our experiments has been described in detail [1, 2]. In the present measurements with C^{6+} and C^{4+} ions, three collimators with apertures of 6–8 mm diameter were installed immediately upstream from the MCP in order to avoid the injection of scattered electrons produced within the spectrometer housing into the MCP. Besides, in the present measurements of low-energy electrons ($<$100 eV) with C^{6+} ions, the cooling cover was changed to that made of μ-metal in order to suppress the effects of stray magnetic fields. The total systematic errors were estimated to be ±13% for all measured angles and energies, while the statistical errors were of the order of 1% at energies smaller than 100 eV and reached several ten % at ∼10 keV.

3. Theoretical model

Calculations of single ionization cross sections for C^{6+} ions were made using the CDW-EIS into its straight-line version of the impact parameter approximation [5]. This model has been used with success in the calculation of single ionization cross sections of water molecules by heavy-ion impact [6–8]. The model takes into account the long-range Coulomb interactions between the collision aggregates in the entry and exit channels. To avoid difficulties associated with the treatment of multielectronic targets, the reaction is reduced to a one-active-electron description. Then, in the entry channel it is considered that the projectile field distorts the initial active-electron orbital with a multiplicative continuum eikonal phase, while in the exit channel the fact that the emitted electron travels in the combined fields of the residual target and projectile is taken into account. Thus, this electron is described as a double product of a plane wave and two Coulomb continuum factors associated with the projectile and residual potentials.

The calculation of the ionization cross sections corresponding to the different molecular orbitals of the water molecule is done within the complete neglect of the differential overlap (CNDO) method. In this approximation (which takes partly into account the molecular character of the target), the ionization cross section for each molecular orbital is calculated by making a linear combination of atomic cross sections, whose weight coefficients are obtained from a population analysis. The characteristics of the molecular orbitals in the gas phase are introduced through their molecular binding energies, instead of using separately those of the atomic compounds of the target. The oxygen atomic orbitals employed in this linear combination correspond to the Slater orbitals of the isolated atom.

4. Results and discussion

4.1. DDCS

Figure 1 shows the energy spectra of DDCSs obtained in collisions of 6.0 MeV u^{-1} C^{6+} and C^{4+} ions with water vapor at angles between 20° and 160° by 10° steps. For both C^{6+} and C^{4+} ions, binary-encounter peaks were clearly observed at the several keV region for angles smaller than 90°, as well as the K-LL Auger peak of oxygen at ∼500 eV for all angles. In addition to these peaks, the DDCSs of C^{4+} ions showed peaks of the electron loss to the continuum (ELC) at ∼3.3 keV particularly at the forward angles. In the low- and intermediate-energy region ($<$400 eV), the DDCSs of C^{4+} ions were observed to be smaller than those of C^{6+} ions by ∼50% due to the screening effect of the bound electrons in C^{4+} ions. A quantitative analysis for the screening effect taking account of an effective projectile charge is described later.

Theoretical calculations of the DDCSs were made for C^{6+} ions using the CDW-EIS approximation for target ionization into its straight-line version of the impact parameter approximation. As can be seen in figure 1, fairly good agreement with measured data is obtained for emission energies smaller than 50 eV. However, the observed DDCSs of C^{6+} ions disagree with the CDW-EIS ones in the intermediate- and high-energy region ($>$50 eV), mainly due to the fact that contributions from Auger emission are not included in the present calculations. This effect appears to be more pronounced at the backward angles ($>$110°). A similar tendency has also been clearly observed in the previously measured DDCSs with 6.0–10.0 MeV u^{-1} He^{2+} ions [1, 2], which seems to be common in other data of low-energy H^{+} (0.3–1.5 MeV) and He^{2+} (0.3–0.5 MeV u^{-1}) ions on the same target (water vapor) [9]. Two-active-electron CDW-EIS calculations for impact of C^{4+}, which must include projectile ELC and simultaneous electron emission from both aggregates of the collision system, are in progress.

4.2. SDCS

Figure 2 shows the energy spectra of SDCSs obtained in collisions of 6.0 MeV u^{-1} C^{6+} and C^{4+} ions with water vapor, which were deduced from the measured DDCSs by integration with respect to the ejected angle. The observed SDCS of 6.0 MeV u^{-1} C^{6+} ions was compared with the CDW-EIS and a simple Z^2 scaling (×36) of the Rudd model. The Rudd model is based on both the molecular promotion model applied to electron emission by low-energy ions and the classical binary-encounter approximation at high energies, so as to agree with the Bethe theory on ionization. Although this model was basically derived from experiments with protons having energies of 5–5000 keV, it has been widely accepted to be applicable to other bare projectiles by Z^2 scaling. In the energy range of 1–200 eV, our SDCS agreed well with the CDW-EIS, and both of them were smaller than the Rudd-model scaling by ∼22% at maximum. In contrast, the previously measured SDCSs with 6.0–10.0 MeV u^{-1} He^{2+} ions were quite consistent with the Rudd-model scaling (×4) in the low-energy region ($10\,\mathrm{eV} < E < 100\,\mathrm{eV}$). This suggests that a simple Z^2 scaling of the

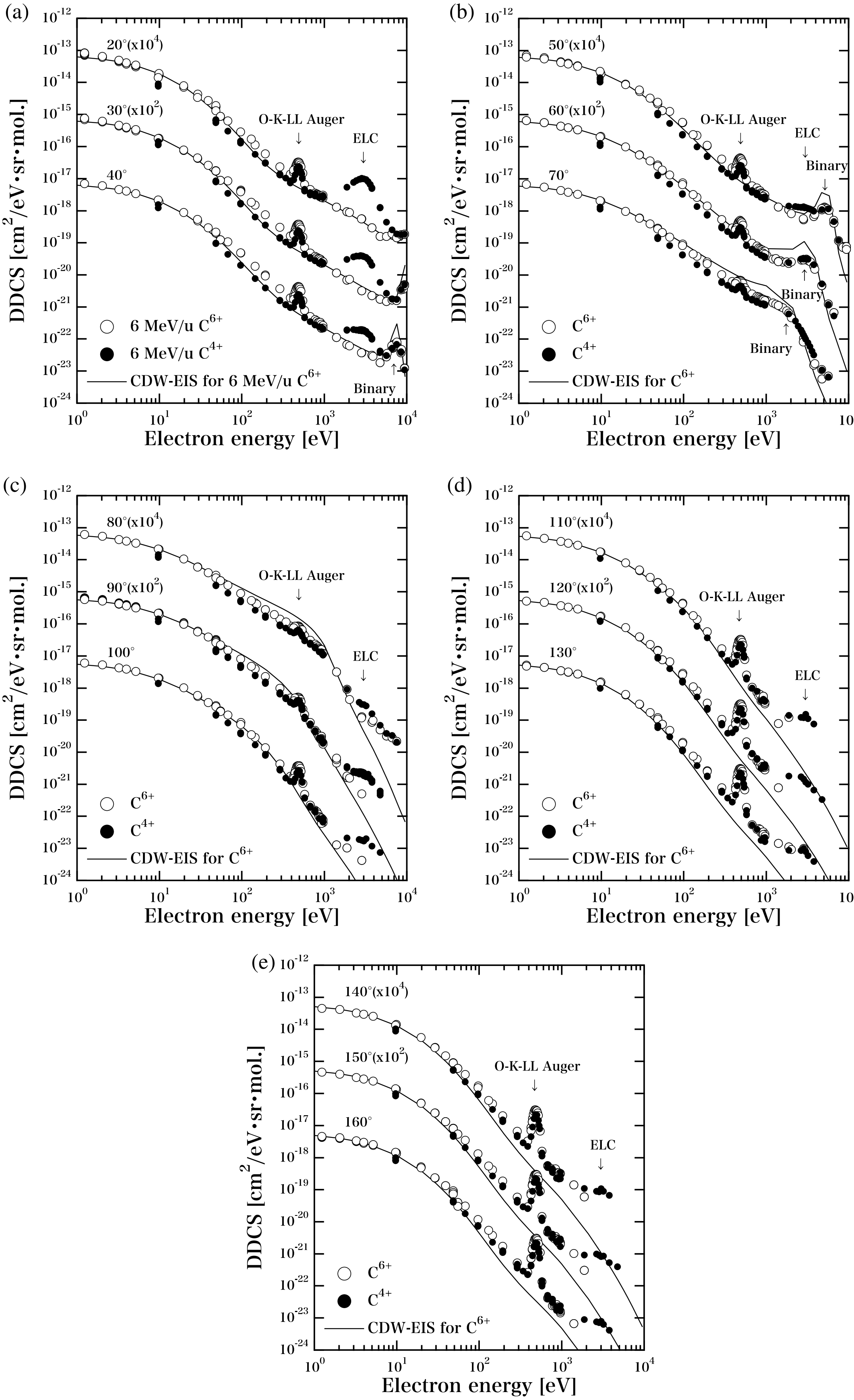

Figure 1. (a)–(e) Energy spectra of DDCSs obtained in collisions of 6.0 MeV u^{-1} C^{6+} (○) and C^{4+}(●) ions with water vapor at angles between 20° and 160° by 10° steps. The solid line shows the CDW-EIS calculated for 6.0 MeV u^{-1} C^{6+} ions. The contributions of K-LL Auger peaks of oxygen, which were clearly observed at ~500 eV for all angles, are not included in the present theoretical calculations.

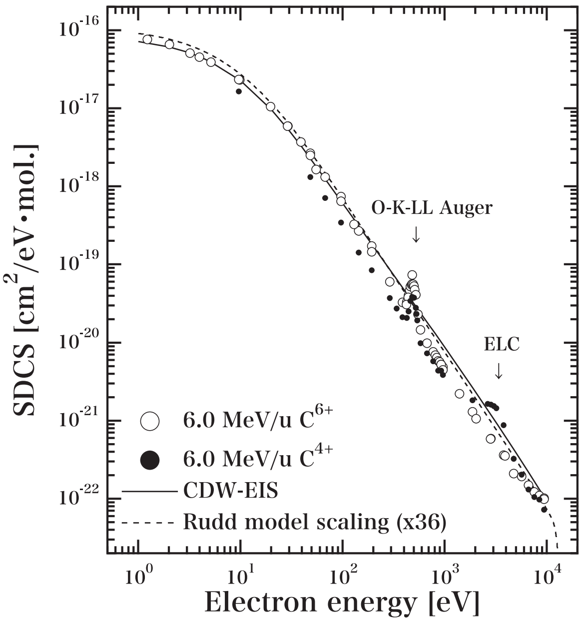

Figure 2. Energy spectra of SDCSs obtained in collisions of 6.0 MeV u^{-1} C^{6+}(○) and C^{4+}(●) ions with water vapor, which were deduced from the measured DDCSs by integration with respect to the ejected angle. The solid and dashed lines show the CDW-EIS and a simple Z^2 scaling (×36) of the Rudd model, respectively.

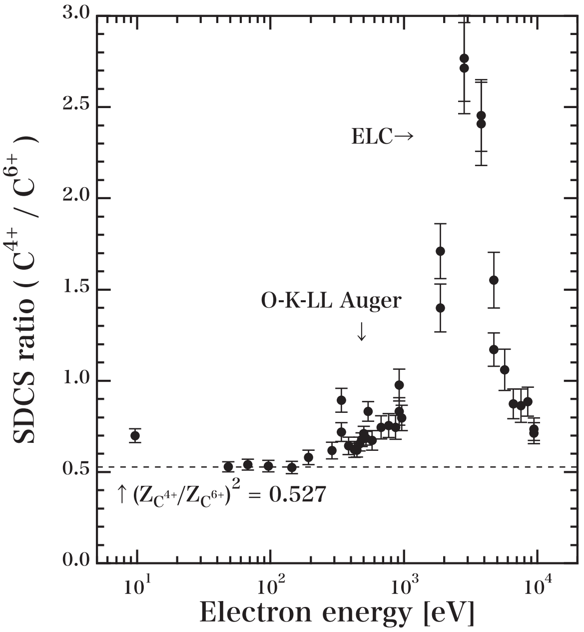

Figure 3. SDCS ratio between C^{4+} and C^{6+} ions as a function of electron energy. The ratio exhibited a nearly constant value around 0.5 in the low-energy region of 50–200 eV along with a pronounced peak due to the ELC at ~3.3 keV. The dashed line represents the square of the effective-charge ratio between C^{4+} and C^{6+} ions.

Rudd model is not sufficient to describe the experimental data for high-Z bare projectiles such as C^{6+} ions. In the energy range of 300 eV–7 keV, compared with the CDW-EIS, our SDCS showed a meaningful reduction by ~50% at maximum at 2 keV, which was also quite consistent with our previous measurements with 6.0–10.0 MeV u^{-1} He^{2+} ions.

In figure 3, the SDCS ratio between C^{4+} and C^{6+} ions was shown as a function of electron energy in order to discuss the screening effect quantitatively, where the ratio was nearly constant around 0.5 in the low-energy region of 50–200 eV. In fast ion–atom collisions, ionization processes occurring with large impact parameters (small momentum transfer) can be treated based on the well-known perturbation theory. According to the theory, the SDCS in the low-energy region is expected to be proportional to the square of the projectile charge. Note here that in the case of the dressed projectile, the effective projectile charge Z_{eff} should be used instead of the real charge. The Z_{eff} of the dressed projectile is generally expressed as

$$Z_{\text{eff}} = \left(\frac{n^2 E_{\text{b}}}{13.6}\right)^{1/2}, \tag{1}$$

where n is the principal quantum number of the electron in the projectile and E_{b} is its binding energy [10]. Using equation (1), the effective charge of C^{4+} ions is found to be

$$Z_{C^{4+}} = \left(\frac{2^2 \times 64.5}{13.6}\right)^{1/2} = 4.36. \tag{2}$$

Thus, the square of the effective-charge ratio between C^{4+} and C^{6+} ions is calculated to be

$$\left(\frac{Z_{C^{4+}}}{Z_{C^{6+}}}\right)^2 = \left(\frac{4.36}{6}\right)^2 = 0.527. \tag{3}$$

As can be seen in figure 3, the SDCS ratio agreed well with the square of the effective-charge ratio in the low-energy region (<200 eV) except at 10 eV within the overall errors, indicating that the approach based on the perturbation theory taking account of the effective projectile charge is valid. We believe the discrepancy at 10 eV may be attributed to an unwanted increase in the residual magnetic field in the measurements with C^{4+} ions.

5. Conclusion

Further improving our previous apparatus, we have successfully measured absolute DDCS and SDCS for secondary electron emission from water vapor by the impact of 6.0 MeV u^{-1} C^{6+} and C^{4+} ions within total systematic errors of ±13%. Comparison of the observed DDCS of C^{6+} ions with the CDW-EIS showed that experiments and theory are in good agreement at low–intermediate emission energies but also revealed that there were significant discrepancies concerning electron emission at the backward angles larger than 110°, especially in the high-energy region. Such discrepancies were similar to other data of low-energy H^+(0.3–1.5 MeV) and He^{2+}(0.3–0.5 MeV u^{-1}) ions on the same target (water vapor), suggesting the necessity of systematic measurements with other projectiles. Also the consideration of Auger contributions in the theoretical model as well as a more complete description of backscattering processes in CDW-EIS appear to be necessary. In the near future, experiments with O and Ne ions will be carried out, after installing a compact 10 GHz ECR ion source to the axial injection line of the cyclotron. Recently, we also developed an event-by-event Monte-Carlo track structure code for He and C ions in water, in which our experimental DDCS and SDCS data were used. Details of it will soon be published elsewhere.

Acknowledgments

We are grateful to the cyclotron staff at NIRS for providing steady beams during the experiments. The work was partially supported by a Grant-in-Aid for Scientific Research Contract(C) no. 21540408 from the Ministry of Education, Science, Sports and Culture of Japan.

References

[1] Ohsawa D, Kawauchi H, Hirabayashi M, Okada Y, Honma T, Higashi A, Amano S, Hashimoto Y, Soga F and Sato Y 2005 *Nucl. Instrum. Methods* B **227** 431–49
[2] Ohsawa D, Sato Y, Okada Y, Shevelko V P and Soga F 2005 *Phys. Rev.* A **72** 062710
[3] Champion C, Boudrioua O, Cappello C D, Sato Y and Ohsawa D 2007 *Phys. Rev.* A **75** 032724
[4] Cappello C D, Champion C, Boudrioua O, Lekadir H, Sato Y and Ohsawa D 2009 *Nucl. Instrum. Methods* B **267** 781–90
[5] Fainstein P D, Ponce V H and Rivarola R D 1988 *J. Phys. B: At. Mol. Opt. Phys.* **21** 287–99
[6] Olivera G H, Martinez A E, Rivarola R D and Fainstein P D 1995 *Radiat. Res.* **144** 241–47
[7] Olivera G H, Fainstein P D and Rivarola R D 1996 *Phys. Med. Biol.* **41** 1633–47
[8] Fainstein P D, Olivera G H and Rivarola R D 1996 *Nucl. Instrum. Methods* B **107** 19–26
[9] Bernal M A and Liendo J A 2007 *Nucl. Instrum. Methods* B **262** 1–6
[10] Pal'chikov V G and Shevelko V P 1995 *Reference Data on Multicharged Ions* (Berlin: Springer)